

## Insights into the Aftershocks and Inter-Seismicity for Some Large Persian Earthquakes

M. Nemati\*

*Department of Geology, Faculty of Science, Shahid Bahonar University of Kerman, Kerman City,  
Islamic Republic of Iran  
Earthquake Research Center, Shahid Bahonar University of Kerman, Kerman City, Islamic Republic of  
Iran*

Received: 8 July 2014 / Revised: 23 September 2014 / Accepted: 14 December 2014

### Abstract

This paper focuses on aftershocks behavior and seismicity along some co-seismic faults for large earthquakes in Iran. The data of aftershocks and seismicity roughly extracted from both the Institute of Geophysics the University of Tehran (IGUT) and International Seismological Center (ISC) catalogs. Apply some essential methods on 43 large earthquakes data; like the depth, magnitude as well as the aftershock data; resulted knowledge about some relations between earthquake characteristics. We found ~16.5km for deep seated co-seismic fault length for the 2005 Dahouieh Zarand earthquake ( $M_W$  6.4) considering the dimension of the main cluster of aftershocks. Moreover, a slightly decrease in aftershocks activity was observed with increase in depth of the mainshocks for some Iranian earthquakes. Also the clustered aftershocks for the 1997 Zirkuh-e Qaen earthquake ( $M_W$  7.1) showed a clear decrease in maximum magnitude of the aftershocks per day elapsed from mainshock. Finally, we could explore an anti-correlation between aftershocks distribution and post microseismicity along co-seismic faults for both Dahouieh and Qaen earthquakes.

Keywords: Aftershock; Mainshock; Magnitude; Seismicity and Persia.

### Introduction

The Iranian plateau has experienced a considerable number of historical, pre-instrumental and instrumental large earthquakes, e.g. the 1930 Salmas ( $M_b$  7.3) and 1962 Buyin Zahea ( $M_S$  7.2) destructive events [49] without instrumental data and 1990 Roudbar-Tarom ( $M_S$  7.7) and 1997 Zirkuh-e Qaen ( $M_W$  7.2) modern earthquakes, which make Iran a significant area suitable for experimental studies.

Large earthquakes are always followed by aftershocks which spatially start clustering around

mainshock hypocenter immediately after the earthquake occurrence. In reality, all of the large earthquakes are associated with aftershocks. The aftershocks generally have smaller magnitude and originate from rupture zone of the mainshock [51]. In most of the earthquakes, the aftershocks are essentially responsible for growth of the co-seismic rupture which is initiated from the mainshock area. In fact, some of earthquakes occur without foreshocks but almost all of large events are followed by numerous aftershocks. They occur shortly after the mainshock and are

\* Corresponding author: Tel. and Fax: +983433222035; Email: majid\_1974@uk.ac.ir

subsequently triggered from immediate vicinity of the focal area. Maybe the aftershocks are a conclusion from strain re-balancing on either main rupture or near pre-existing minor faults, e.g. [26].

In an inter-seismic chronically period, each seismically active area experiences a steady-state background seismicity. It is generally referred to as microseismicity. It also discharges routine seismic stress which is a consequence from the regional or local tectonism in the area. Following occurrence any moderate and large earthquakes at the environment of background seismicity, aftershocks activity will be a recovery response to change in the seismic stress. The seismic stress regime is globally disturbed by the mainshock near the fault plane and also in around area.

In subduction zones, because of relative ductile rheology of sinking plate, the deep events could not produce so many aftershocks. There are worldwide investigations, e.g. [27], which introduce relationships for aftershocks depth of the continental earthquakes. Likely, at the Persian plateau the earthquakes, aftershocks as well as microseismicity occur rarely deeper than ~25km, e.g. [16] for the eastern Iran; [38] for the Zagros; [31] for the Alborz) except in the

Makran, e.g. [12] and north of the Alborz, e.g. [13]. Considering the average geothermal gradient ( $\sim 30^{\circ}\text{C.Km}^{-1}$ ) for crustal structure in Iran, the strength of the continental crust which gradually increases with depth, starts to decrease at ~15km depth. The strength of this depth which is equivalent to a stress value of ~400MPa closes to zero at the Moho depth [25]. Notwithstanding above hypothesis, we expect more than 15km for the maximum earthquakes depth dispersal at least in Iran. As typical examples in Persia, we could point to 15km for majority of earthquakes depth for the eastern Alborz and also Azarbayjan [31, 28], less than 20km for the eastern Iran [39, 31] and 15km for the Zagros [38, 47]. Mogi, 1962 has also investigated the dependence of aftershocks activity to the mainshock focal depth. He demonstrated that the probability of occurrence at least 20 aftershocks ( $M>3.0$ ) for 10km for depth of mainshock is 80% whereas, it decreases to 10% for 60km for mainshock focal depth. Considering the fact that it depends on magnitude of the mainshock, the Mogi's rule could not be used as a definite rule instead, it only could be used as a general guide for the earthquakes and the related aftershocks in the seismological interpretations.

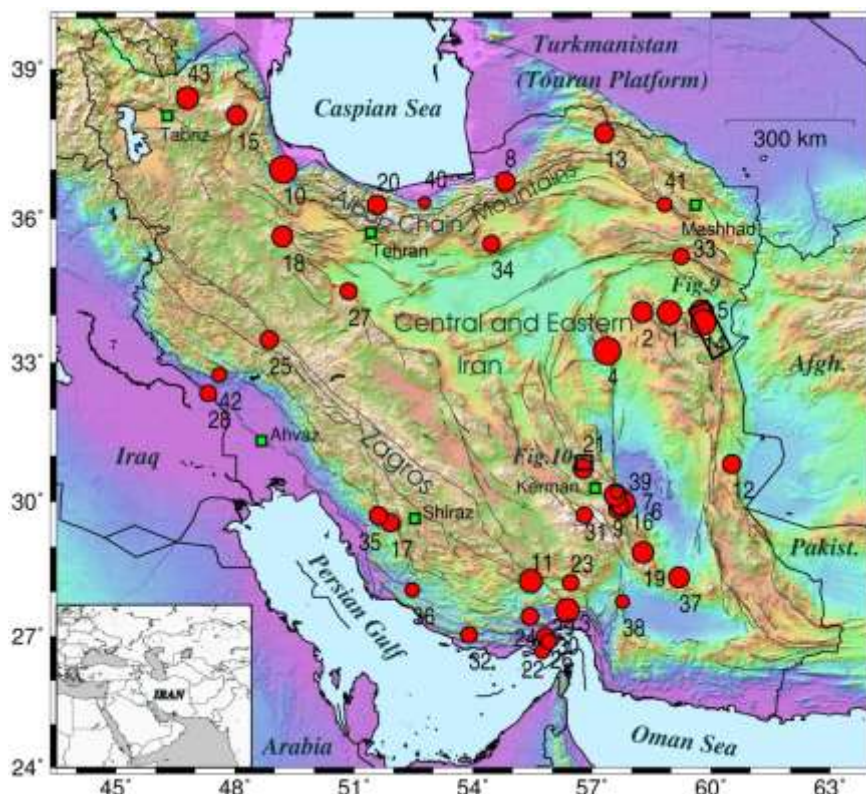


**Figure 1.** Large earthquakes (circles) which have occurred in the Alborz-Azarbayjan, Kopeh Dagh, Zagros and eastern Iran seismotectonic provinces. The inset map shows the Middle East and around and the green rectangles display locations for the major cities in Iran. The faults adapted from Iranian active fault map [21]. The open rectangles display locations for the Fig. 9 and 10.

Usually materials which construct shallower crustal structure are not too strong to accumulate enough elastic strain energy for creation a rupture. Also ruptures and fractures for the microearthquakes do not have outcrop in earth surface because of both ductile rheology of sedimentary cover and also small magnitudes for the microearthquakes. Always there are remarkable numbers of microearthquakes which are not associated with a recognized surface trace of a particular active fault. Instead they could be sources for blind faults which affect the basement crystalline

crust (e.g. in southeast of the Caspian Sea [32, 33] and in south of Tehran [1], The Caspian name comes from people of Caspi pedigree who inhabited in the Qazvin city [50]).

Several researchers focused on the distance between mainshock and their largest aftershocks in a main cluster which is formed near the mainshock, considering the fact that mainshock-aftershock sequence may not be valid for deep earthquakes even for large events. Hosono and Yoshida, (1991) have demonstrated that the distance between the largest

**Table 1.** The earthquakes used in this study. Locations are from the Engdahl Catalogue [54].

No	Earthquake Name	Date	Origin Time	Magnitude	Latitude (°N)	Longitude (°E)
1	Dasht-e Bayaz	31/08/1968	10:47:00	$M_w=7.1$	34.050	58.950
2	Ferdows	01/09/1968	07:27:00	$M_w=6.5$	34.070	58.270
3	Khorgu Bandar-e Abbas	21/03/1977	21:18:54	$M_w=7.0$	27.588	56.379
4	Tabas-e Golshan	16/09/1978	15:35:58	$M_s=7.7$	33.244	57.384
5	Kouli-Boniabad	27/10/1979	17:10:00	$M_w=7.1$	34.060	59.760
6	Golbaf	11/06/1981	07:24:24	$M_w=6.6$	29.855	57.687
7	Sirch-1	28/07/1981	17:22:24	$M_s=7.3$	29.966	57.767
8	Ali Abad-e Gorgan	20/10/1985	13:13:40	$M_w=6.4$	36.750	54.810
9	Sirch-Golbaf	20/11/1989	04:19:07	$M_w=5.9$	29.901	57.712
10	Roudbar-Tarom	20/06/1990	21:00:10	$M_s=7.7$	37.002	49.219
11	Darab-e Hormozgan	06/11/1990	18:46:00	$M_s=6.9$	28.240	55.461
12	Sefidabeh	24/02/1994	08:02:00	$M_w=6.2$	30.821	60.529
13	Garmkhan-e Bojnourd	04/02/1997	10:37:00	$M_w=6.4$	37.728	57.310
14	Zirkuh-e Qaen	10/05/1997	0.33125	$M_s=7.3$	33.844	59.811
15	Ardebil	04/07/1997	16:27:17	$M_s=6.4$	38.088	48.041
16	Fandogha	14/03/1998	19:40:28	$M_s=6.7$	30.138	57.586
17	Central Zagros	06/05/1999	23:00:00	$M_w=6.1$	29.534	51.917
18	Changoureh Avaj	22/06/2002	02:58:00	$M_w=6.5$	35.636	49.199
19	Bam	26/12/2003	01:56:52	$M_w=6.6$	28.882	58.288
20	Baladeh Kojour	28/05/2004	12:38:42	$M_w=6.4$	36.281	51.582
21	Dahouieh Zarand	22/02/2005	02:25:20	$M_w=6.4$	30.721	56.775
22	Qeshm-1	27/11/2005	11:13:00	$M_w=5.4$	26.748	55.827
23	Haji-Abad-e Hormozgan	28/02/2006	07:31:09	$M_N=5.8$	28.205	56.462
24	Bandar-e Abbas	24/03/2006	07:29:00	$M_N=6.0$	27.451	55.440
25	Darb Astaneh-e Boroujerd	31/03/2006	01:17:04	$M_N=6.1$	33.483	48.864
26	Qeshm-2	28/06/2006	21:02:00	$M_N=5.5$	26.665	55.747
27	Qom	18/06/2007	11:00:00	$M_N=5.9$	34.498	50.866
28	Shoush	27/08/2008	21:52:40	$M_N=5.8$	32.344	47.325
29	Qeshm-3	10/09/2008	11:00:00	$M_N=6.0$	27.002	55.829
30	Qeshm-4	07/12/2008	13:36:00	$M_N=5.6$	26.884	55.909
32	Ashknan-Fars	20/07/2010	19:38:12	$M_N=5.8$	27.040	53.899
33	Torbat-e Heydarieh	30/07/2010	13:50:13	$M_N=5.7$	35.222	59.252
31	Negar-Kerman	31/07/2010	06:52:57	$M_N=5.8$	29.703	56.812
34	Touchahi-Damghan	27/08/2010	19:23:49	$M_N=5.9$	35.488	54.466
35	Kazeroun	27/09/2010	11:22:47	$M_N=6.1$	29.693	51.618
36	Firouz Abad-Fars	26/11/2010	12:33:40	$M_N=5.4$	28.040	52.473
37	Rigan-Balouchestan	20/12/2010	18:41:58	$M_w=6.5$	28.330	59.194
38	Kahnooj	15/06/2011	01:05:30	$M_N=5.3$	27.784	57.766
39	Sirch-2	26/06/2011	19:47:00	$M_N=5.2$	30.206	57.630
40	Marzicola-Mazandaran	11/01/2012	17:08:00	$M_N=5.0$	36.329	52.781
41	Neyshabour	19/01/2012	12:46:58	$M_N=5.5$	36.288	58.835
42	Bostan	03/05/2012	10:09:37	$M_N=5.5$	32.738	47.605
43	Ahar-Varzaghan	11/08/2012	12:23:15	$M_N=6.8$	38.433	46.806

aftershocks and mainshock is positively correlated to the earthquake fault length for the Japanese events. Afterwards this method was also developed by Nanjo and Nagahama, (2000). Using this method, they could specify rupture length for two moderate earthquakes (1984/9/14 Nagano-Ken and 1984/8/6 Unzen events) in Japan.

In this paper we examined 43 Persian earthquakes in order to obtain rupture length and relationship between both magnitude and depth of mainshock with number of aftershocks. The relation between magnitude and time decay of aftershocks and comparing between interseismic seismicity and aftershocks distribution along co-seismic ruptures for some events were also investigated. Here we take a glance to some major destructive earthquakes (Table 1 and Figure 1) which attracted much scientific attentions.

### Materials and Methods

#### *The 1978 Tabas-e Golshan earthquake*

The 1978/9/16 Tabas-e Golshan earthquake was the most devastating earthquake in Iran. Co-seismic fault for this earthquake was 80km discontinued rupture with a NW-SE direction on foothills of the Shotori Mountains at the eastern Iran. According to that the well located aftershocks which could basically specify the geometry of the fault at the base of seismogen layer, if the fault behaves as a listric fault (e.g. 1978 Tabas earthquake) or steepens to the lower crystalline crust (e.g. 1971 San-Fernando earthquake, USA, dip of  $10^\circ$  for fault plane at surface and  $52^\circ$  at 8.4km depth) [3, 4]. The aftershocks for the Tabas event recorded with the criteria of  $RMS < 0.2s$  and horizontal and vertical errors  $< 2$  km for which at least 5P and 3S readings and located using a 3-layer crustal model with a dense station distribution [3, 4]. Some researchers, e.g. [48], believe that a brittle ductile or pure ductile layer sandwiched between brittle upper crust and the upper mantle is responsible for flattening the faults in basement of the crust. The Tabas earthquake with a thrust mechanism was a seismological response to the Shotori Mountains elevating [41].

#### *The 1990 Roudbar-Tarom earthquake*

The Roudbar-Tarom earthquake is one of the continental mega earthquakes ( $M_S$  7.7) which has ever occurred in Iran (at the western Alborz) during the instrumentally period. The 1990/6/20 Roudbar earthquake, which is a clear example for bilateral behavior for the co-seismic fault has ruptured the earth surface in three separated segments (Baklor, Kabateh and Zardalu) with a total length of 80km. The co-

seismic rupture was a right-stepping, left-lateral and steep south dipping fault [7, 10]. According to waveform modeling with a method which has generated mechanisms similar to the Harvard Un. CMT solution, the centroid depth of the earthquake has been obtained between 13 and 15km [7, 15]. Based on a local network data deployed by the IGUT, depth dispersal of the aftershocks reaches maximum to 20km [52].

#### *The 1997 Garmkhan-e Bojnourd earthquake*

The 1997/2/4 Garmkhan-e Bojnourd earthquake is the last instrumentally earthquake with  $M_W > 6.0$  which has occurred at the Kopeh Dagh seismotectonic province at northeast of Iran. Notwithstanding there was not any surface mature rupture related to the Garmkhan-e Bojnourd earthquake ( $M_W$  6.4, [20]), the locally recorded aftershocks have been extended 25km in surface and 20km in depth and showed a NNW-SSE direction with a right lateral strike slip motion for the causative fault [17, 20]. Hollingsworth, et al., 2007 also explored a probable directivity for this earthquake in which the earthquake rupture has nucleated at the north and propagated to the south.

#### *The 1997 Zirkuh-e Qaen earthquake*

The right lateral strike slip and steep dipping Abiz fault (~N-S trending) at the east of Iran was host of a destructive earthquake at the east of Persia, the 1997/5/10 Zirkuh-e Qaen earthquake. Aftershock distribution [16] as well as field observations [6] for the Zirkuh event ( $M_W$  7.2) revealed that the co-seismic rupture and aftershocks elongation of this event were about 125 and 95km respectively. It is the longest co-seismic rupture which has ever been produced and mapped in Persia in the modern history of seismology. Berberian, et al., (1999) have calculated a strike slip mechanism using body waveform modeling and have measured maximum 2m for surface slip for this earthquake. Aftershocks spatial distribution demonstrated that the causative co-seismic fault have had steep dipping and extended to maximum 20km depth. Considering the aftershocks distribution relative to the mainshock epicenter, it is concluded that the rupture has initiated at the NNW and extended to the SSE in a unilateral manner [16].

#### *The 2003 Bam earthquake*

The 2003/12/26 Bam earthquake ( $M_W$  6.6) which has occurred at southeast Iran is an urban destructive earthquake and killed about 26,000 bodies (the official declaration) during tremors. The Bam event aftershocks had N-S trending with 25km elongation

and showed a right-lateral strike-slip mechanism [39, 22]. Following a precisely aftershock surveying with a dense seismological network (IIIES), Tatar, et al., (2005) reported that the aftershocks depth dispersal for the Bam earthquake is 6-20km. The researchers are still debating about the causative fault for this event, because the aftershocks distribution was associated with both the co-seismic rupture and pre-existing the Bam-Baravat fault. The Bam-Baravat thrust fault is associated with a folding at surface which is still well preserved by the nature and known as the Bam-Baravat escarpment. Jackson, et al., (2006) believed that the co-seismic slip for the fault at depth reaches to 2m.

#### ***The 2004 Baladeh Kojour earthquake***

A rare example from intercontinental moderate earthquakes in Persia has occurred in 2004 on the south of the Caspian Sea on the Caspian (Khazar) reverse fault. The Baladeh Kojour earthquake (2004/05/28,  $M_w$  6.4) aftershocks lied between 10 and 30km in depth and elongated 25km in surface. Using body waveform modeling method, near 22km depth with a thrust mechanism as well as a  $34^\circ$  south dipping plane were fitted to the active plane for the mainshock. That was not an ordinary continental earthquake because properties of plate margin earthquakes are seen in the source parameters like mechanism, depth as well as the seismic stress drop [40, 53]. Moreover, the eastern Caspian fault has also been recognized as responsible for the 1985 Ali Abad-e Gorgan earthquake ( $M_w$  6.4) which likely showed foot prints from an interplate earthquake [32]. Donner, et al., 2013 demonstrated that the mainshock and some aftershocks for the Baladeh event show dominant thrust mechanisms at depths between 14 and 26km, with NW–SE striking fault planes and also the mainshock ruptured a  $28^\circ$  south-dipping fault of  $24 \times 21$ km.

#### ***The 2005 Dahouieh Zarand earthquake***

The 2005/2/22 Dahouieh Zarand earthquake has occurred on an E-W new born and reverse rupture with a partially right-lateral strike-slip component. This intramountain earthquake was severely occurred following right-lateral motion of the Kuhbanan giant fault with NW-SE trending at the east of Iran [37, 31]. Talebian, et al., (2006) calculated a dominant thrust mechanism with a partial right lateral strike slip component with a near E-W directed and north dipping ( $\sim 60^\circ$ ) for the active plane for this event. They also mapped the co-seismic rupture with about 13km (continuous) elongation and also  $60-80^\circ$  north dipping fault. When an earthquake occurs on a reverse fault, especially on an immature and hidden fault, the

hanging wall will be recognized as the block including most of the aftershocks and the fault trace could roughly be supposed as a line which limits the aftershocks surficially. This phenomenon partially happened during the 2005 Zarand event and for its locally recorded aftershocks sequences [31]. Nemati and Gheitanchi, (2011) reported about 20km and 25km for depth dispersal and also surface extension of the locally recorded aftershocks respectively.

#### ***Data collection***

We have analyzed the data extracted from both the Institute of Geophysics, the University of Tehran (IGUT, [55]) and International Seismological Center (ISC, [54]) catalogs and the other documented earthquake data. The data is the location, depth and origin time for the foreshocks which have occurred 10 days before and aftershocks which have occurred 60 days after the moderate-large Iranian earthquakes (from 1968 to 2012). The ISC database is used for the earthquakes from 1968 to 2006 and the IGUT database is searched for the events of 2006 to 2012; because the earthquake data before 2006 has been removed from the IGUT website.

The 43 earthquakes (Table 1 and Fig. 1) were carefully selected from all over Iran to ensure that no regional bias and seismotectonical efficacy were included due to the choice of a specific catalog or a specific geological setting. Moreover the mentioned earthquakes have significantly been chosen from the events which mainly were documented either geologically or seismologically. We mainly needed the source and rupture parameters for the earthquakes in order to depict diagrams and make comparison and also interpretation. Neglected earthquakes which were excluded from processing are naturally the events with no accurate and reliable source, rupture and also aftershocks information.

One of the important restrictions for our analysis is the fact that the ISC catalog which gives the most exhaustive list of aftershocks, reports the events in different magnitude scales. Therefore we converted the magnitude scales for the aftershocks to a uniform scale of  $m_b$  using the generated relationship ( $m_b = 0.65M_S + 2.5$ ) by Katsuyuki and Kanamori, (1980).

The data includes 22 earthquakes from the IGUT database which have a magnitude range between 5.0 and 6.8 in  $M_N$  scale and also 21 ISC events ( $M_w$  5.4-7.4, Table 1 and Fig. 1).

A significant issue for this kind of analysis is estimation of the magnitude of completeness ( $M_C$ ) for the databases. The  $M_C$  is reasonably defined based on the magnitude value above which a catalog completely

reports the earthquakes and the catalog could be assumed to be complete. Our estimation for magnitude of completeness is reliably based on the Gutenberg-Richter law [18] which explains a large percentage of the frequency-magnitude distribution above a given completeness magnitude. The percent includes over 0.9 of the data. It is natural that within the first hours to days after a mainshock,  $M_C$  tends to decrease systematically. This is caused by the fact that in the recorded waveforms the larger aftershocks eclipse smaller events in the recorded waveforms during first few days elapsed from mainshock, which experiences numerous aftershocks with time overlapping [11]. In other words, whenever aftershocks rate decreases, the seismological instruments could record the aftershocks separately and hence the catalog will include smaller events. Therefore the catalog becomes more complete and also the  $M_C$  decreases to a smaller value. Hence we include the aftershocks with magnitude greater than the  $M_C$  in data processing.

The ISC catalogue is incomplete in comparison with the IGUT, in other words, less numbers of the ISC aftershocks are available in comparison with the IGUT database. Therefore we do not have any problem with the data which is searched from the IGUT database. The mentioned earthquake data (e.g. mainshocks depths and magnitudes, number of the aftershocks and microseismicity along faults for some earthquakes from the Table 1) before 2006 and also the

information for the events after 2006 are adapted from the ISC and IGUT catalogs respectively. All the diagrams for this paper were calculated and depicted using the Origin software and also GMT [46] software respectively.

### Rupture length

In this section rupture length for the 2005 Zarand earthquake is estimated using both Hosono and Yoshida, (1991) and Nanjo and Nagahama, (2000) invented method. Based on this method the distance between pairs of aftershock-mainshock hypocenters for both the largest and furthers aftershocks which are situated in main cluster of aftershocks controls the rupture length at depth. Only the precisely located aftershocks and also mainshock are essentially included for estimation of the depth rupture with this method. Figure 2 shows the hypocentral distances between every aftershock and mainshock of the Dahouieh earthquake. The depth extension for the Zarand event rupture is obtained about 16.5km which is normally wider than surface rupture. About 13km has geologically been mapped for the surface rupture for this earthquake by Talebian, et al., (2006), considering continuous parts of the rupture. Surprisingly they have also mentioned to the probability of existence of the wider rupture at depth. The aftershocks have been recorded with a local network owned by the IGUT [31]. They located the

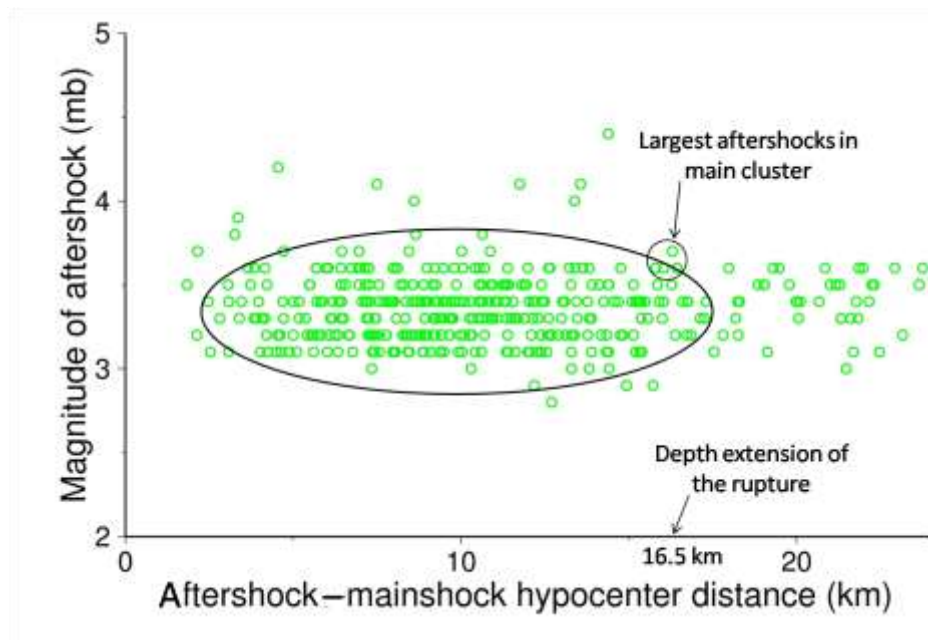


**Figure 2.** Aftershock-mainshock hypocentral distance of the 2005 Zarand earthquake. Location and depth of the mainshock are from the Engdahl catalogue [54] and body waveform modeling [37] respectively and aftershocks are from a local network [31]. Ellipse shows the main cluster of the aftershocks.

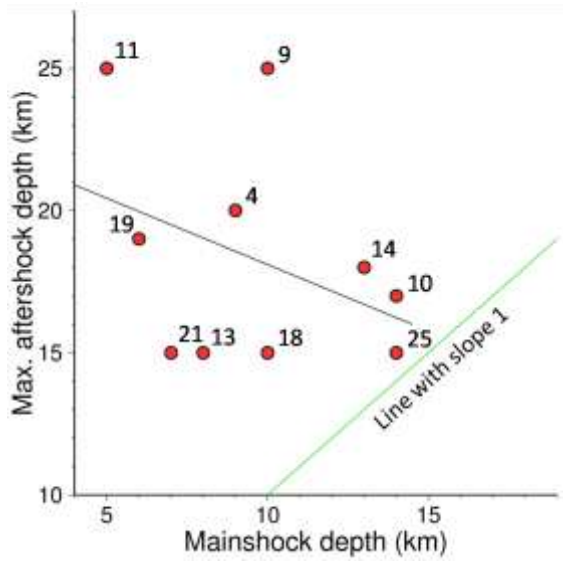


**Figure 3.** Maximum depth for aftershocks versus depth of the mainshock. The black line is fitted using a linear fit method by the Origin software [56] and the line with slope 1 clarifies that none of the mainshocks is deeper than their related aftershocks. The earthquake references are: 4 [3, 4, 41], 9 [9, 5, 14], 10 [52, 7, 10], 11 [42], 13 [20], 14 [6, 16], 18 [43], 19 [22, 39], 21 [31, 37] and 25 [36].

aftershocks with a reasonable accuracy range; the RMS smaller than 0.2s, azimuth gap smaller than 180°, number of read phases for locating greater than 7 and horizontal and vertical errors of locations smaller than km.

**Depth, magnitude and frequency of aftershocks**

Geothermal gradient of the continental crust efficiently limits the brittle and brittle-ductile layers depth and therefore depth range for the earthquake occurrence. In Iran this depth rarely exceeds than 15-25km in various regions. Mogi, (1962) investigated that the aftershocks activity decreases with increase in depth of the mainshock. Within the 10 large investigated earthquakes, the aftershocks maximum depth is not deeper than 25km. For these earthquakes the aftershocks sequences are recorded with dense local seismological networks. Therefore with a high degree of confidence we could say that the aftershocks occurred in around the mainshock location especially for crustal region of meant and none of the mainshocks are deeper than related aftershocks. In Figure 3 we displayed depths for the mainshocks which are adapted from body waveform modeling method (jointly inverted with mechanism determination) versus maximum depths for the aftershocks which are adapted from local networks data. In many researches devoted

to waveform modeling the depth and focal mechanism is jointly inverted and the proper depth is sensitive on proper focal mechanism. Also in this diagram a line is fitted to the symbols with linear method. Neglecting less numbers of the symbols, the negative slop for the line ( $MAD = (-0.427 \pm 0.400) MD + (22.508 \pm 4.03)$ ) confirms a descent in the general trend for the symbols. We see the fact that the aftershocks occur in shallower depth when there are increase in hypocentral depth for the mainshocks.

A global example for dependence of aftershocks

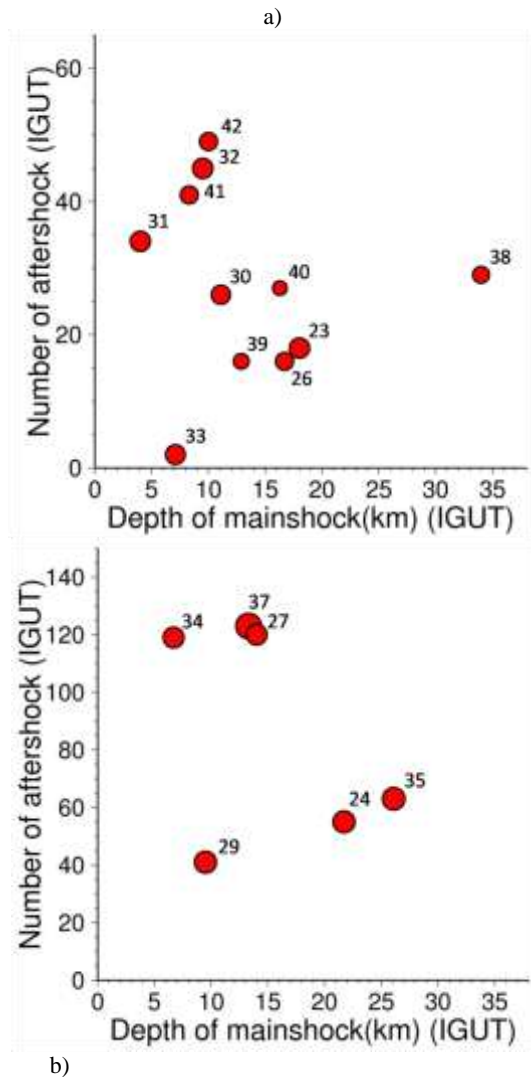


**Figure 4.** Number of aftershocks during 60 days after mainshock versus depth of the mainshock. All of the information presented in both diagrams adapted from the IGUT catalog. If we consider earthquakes with two ranges of magnitude a) 5.0-5.8 and b) 5.8-6.8 and neglecting off-cluster symbols, we will see a decrease in the aftershocks activity with increase in depth of the mainshock.

activity with depth of the mainshock is Mogi, (1962) investigation, which concludes that aftershocks activity decreases with increase in depth of the mainshock. For Iranian earthquakes, number of aftershocks during 60 days after the IGUT mainshocks versus depth of the mainshocks are depicted in Figure 4a and b in two ranges of magnitudes. For both ranges, 5.0-5.8 and 5.8-6.8, and neglecting off-cluster symbols (#29 in Fig. 4a and #33 and 38 in Fig. 4b), numbers of aftershocks decrease with increase in depths of the mainshocks especially in the Fig. 4b. It is important that in these kinds of the diagrams great uncertainty in depth determination makes the distributions are rather random.

Earthquake #29 is 10/9/2008 Qeshm earthquake which is at the southernmost region of Iran. The earthquake and also aftershocks have recorded with greater gap azimuth ( $>180^\circ$ ) by the IGUT seismological network and therefore maybe could not record so many well located aftershocks. A possible interpretation for the event #33 (30/07/2010 Torbat-e Heydarieh event at the eastern Iran) is that if a strike slip fault cut the area of rigid materials, because of rigidity, the rupture zone will be extra narrow and less number of aftershocks occur on this kind of faults (compare the Tabas eq. with a reverse fault zone, [3, 4] with the Zirkuh event with strike slip fault, [17]). Earthquake #38 is 15/06/2011 Kahnooj event which is belonging to the transition zone between the Zagros intraplate and Makran interplate areas. Deep centroid for this earthquake is not an error of location. According to the IGUT catalog all of the earthquakes at that area have depths (max. ~40km) deeper than the others in Iran (max. ~20km).

Figure 5 shows number of aftershocks during 60 days after mainshock versus depths of the mainshocks for the ISC reported events. Because of the problems arisen from magnitude of completeness we could not see a clear relationship between the aftershocks activity with increase in depth of the mainshock, even if we consider the earthquakes with respect to their magnitude ranges. Definitely a higher numbers of the aftershocks are available for a mainshock of greater magnitude. Basically a true relationship is only achieved, whenever the aftershocks for the earthquakes with a same magnitude are only compared with each other. If we consider more earthquake data in a narrow magnitude range, we will see much more explicit relationships. But, lack of the earthquake data in Iran forced us divide the data into two separate magnitude ranges.

In Figure 6 we displayed how a mainshock magnitude affects on aftershocks activity. In this

diagram neglecting off cluster earthquakes (#21, 25 and 30 from the ISC and #27, 33, 34, 36 and 37 from the IGUT database) there is a clear increase in number of aftershocks with increasing in mainshock magnitude

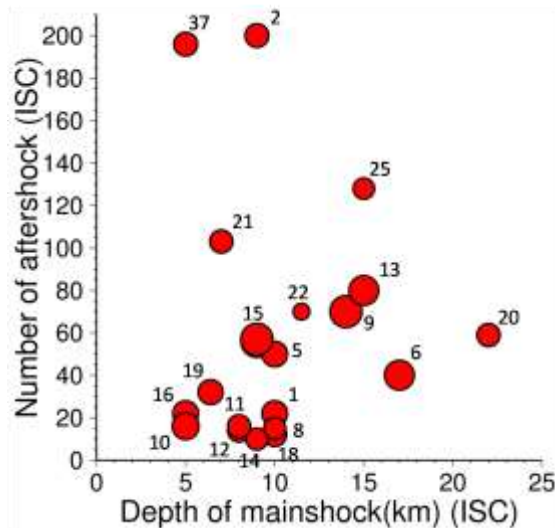


**Figure 5.** Number of aftershocks during 60 days after mainshock versus depth of mainshock for the ISC reported events. Depths of the mainshocks adapted from body waveform modeling. Considering the references for the earthquakes of the Fig. 3, the other events references are: 1, 2 and 5 [44], 6 [9], 12 [8], 15 [2], 16 [9], 22 [34], and 37 [45].

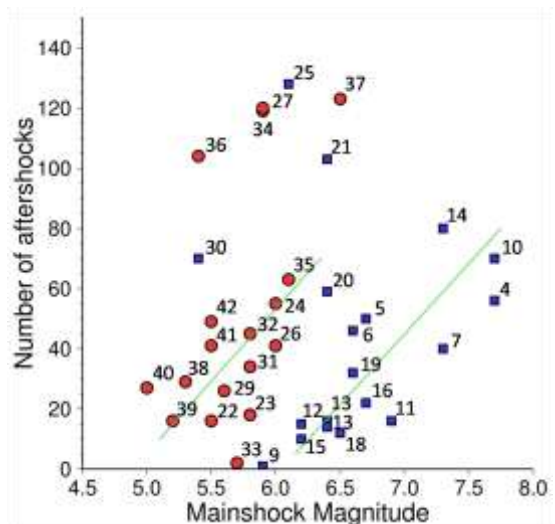


**Figure 6.** Relationship between number of aftershocks and magnitude of their mainshocks for the IGUT (Circle) and ISC (Rectangle) catalogs data. Magnitude scale for the IGUT is  $M_N$  and of the ISC [54] is  $M_W$ . The lines are linear regressions and are depicted using the Origin software [56].



for both the IGUT and ISC data. Both the IGUT (Circle) and ISC (Rectangle) events are shown in a same diagram for a reliable comparison. If we consider a same magnitude value in this diagram, there are much more aftershocks which are reported by the IGUT database rather than the ISC. This problem may come from incompleteness of the ISC catalogue. One of the important reasons for this problem is large station spacing of the ISC seismological network. Although, difference between number of aftershocks which are achieved from a same mainshock magnitude for the two databases may partially come from difference between the magnitude scales for the two catalogues ( $M_N$  for the IGUT and  $M_W$  for the ISC).

**Magnitude decay of aftershocks**

Maximum magnitude of the aftershocks per day versus day elapsed from mainshock is a useful method for clustering the aftershocks for a large earthquake. We collected magnitude-time sequences of aftershocks which were occurred after a major earthquake from the Eastern Iran, the 1997 Zirkuh-e Qaen event. Figure 7 displays two main clusters which are performed by the Zirkuh aftershock sequences. In this diagram, an obvious decrease is seen for the maximum magnitude of the aftershocks per day versus time. This data clearly shows two main separate clusters during almost two months since the mainshock. Five foreshocks are shown 10 days to three days before the event and afterwards three quiet days before the mainshock (10<sup>th</sup> day in the diagram) is seen. Decrease of foreshocks activity and afterwards a few days seismic quiescence is a significant issue which is used as a supplementary material for prediction of earthquakes along active

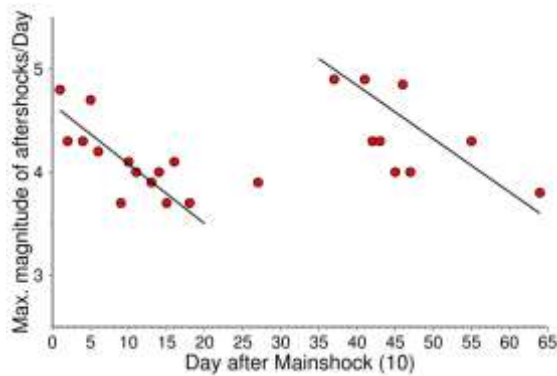


**Figure 7.** Maximum magnitude of the aftershocks (ISC) of the 1997 Zirkuh event per day versus day after mainshock as a way for distinguish clustering in 65 days foreshock and aftershock sequences. The lines were drawn using linear regression with the origin software [56].

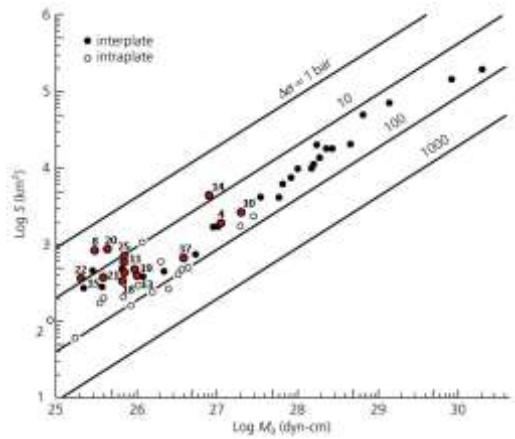


**Figure 8.** Plotting Persian earthquakes on the Kanamori and Anderson, (1975) diagram. The interplate and intraplate earthquakes data which were gathered from all over the world are characterized by solid and open circles respectively. The symbols with numbers are Iranian earthquakes. The cluster which is formed by 4, 10 and 14 events are mega earthquakes ( $M_W > 7.0$ ) and 8 and 20 events are interplate earthquakes (both with  $M_W$  6.4). References for the earthquakes are: 4 [3, 41], 8 [33], 10 [6, 10], [11 43], 13 [20], 14 [6, 16], 15 [2], 18 [43], 19 [39, 22], 21 [31, 37], 22 [35] and 25 [36].

faults. An aftershock with larger magnitude ( $m_b$  4.9) which has occurred 37 days after the mainshock seems to be responsible for the second clustering. It seems that this event may act as an individual earthquake and have its own aftershocks. In other words, instead of considering a single aftershock sequence, two mainshocks with separate aftershock sequences could also be considered for this diagram. The seismic silence between the two clusters (between days of 20 and 37) is a remarkable testimony for this idea.

**Stress drop for the earthquakes**

The scalar moment of the earthquakes are directly proportioned to the faulted area caused by the events, both in logarithmic scales [23]. Plotting earthquakes in this diagram is a useful way for distinguish between plate-margin and mid-plate events because they are substantially distinguishable with respect their stress drops. Scattering of the earthquakes between the lines in this diagram which specify the stress drop of the events guides us generally for categorizing the earthquakes. In Figure 8 we display 13 large Persian intraplate earthquakes (except #8 and 20; the 1985 Ali Abad-e Gorgan and the 2004 Baladeh Kojour earthquakes respectively with interplate behaviors). The stress drop range for the earthquakes is achieved between 5-90bar. The scalar moment for the

earthquakes has been adapted from earthquake CMT solution catalog of the Harvard University. Also the ruptured area is calculated from producing of surface rupture (documented in geological field observation) into the maximum depth of the aftershocks (from local networks data). A main cluster of circles (#11, 13, 15, 18, 19, 21, 22 and 25) is seen from the intraplate earthquakes. The cluster formed by earthquakes #4, 10 and 14 which is completely separated from the others is major earthquakes ( $M_S > 7.3$ ) which Persian plateau ever experienced in modern seismological history. Most importantly, signature of the intercontinental behavior is distinguishable for the earthquakes #8 and 20 which have the lowest stress drops.

#### *Aftershocks and inter-seismicity*

Along any active fault, we could be able to compare recent microseismicity only with the latest earthquake aftershocks distribution, because the large earthquakes completely disturb stress regime of the environment along the fault. Therefore aftershocks activity and subsequent background seismicity which are occurred on or near any active fault, which are projected on the fault plane, should not have overlapping with each other. Therefore it is expected that the area with dense accumulation of aftershocks is correlated with the empty area of background seismicity.

Scholz, (2002), demonstrated this phenomenon for large earthquakes in America. The 1997 Zirkuh ( $M_W$  7.2) earthquake is a clear evidence for this

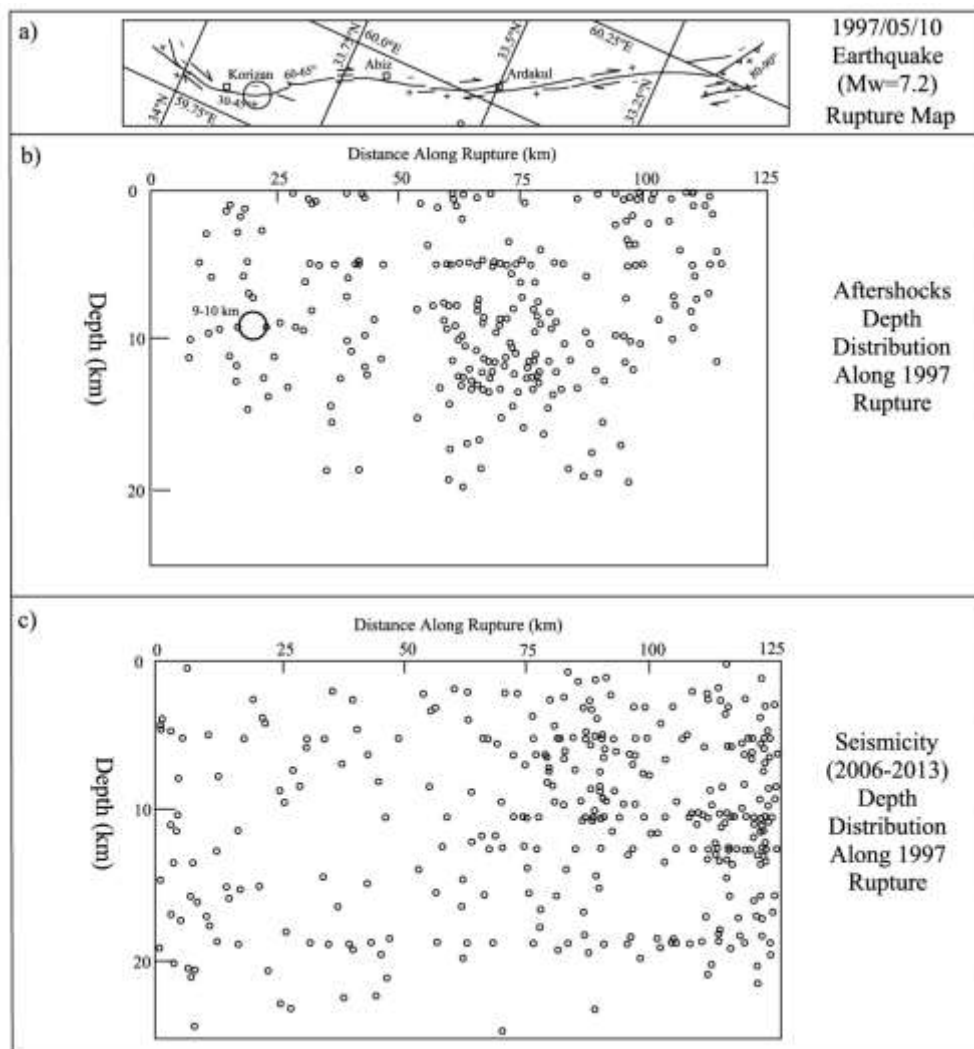


**Figure 9.** a) The 1997 Zirkuh earthquake co-seismic rupture [6], b) the Zirkuh aftershock sequence [16] and c) microseismicity (IGUT) along 1997 earthquake fault. The hypocentral area is empty from aftershocks and is still empty from microseismicity.

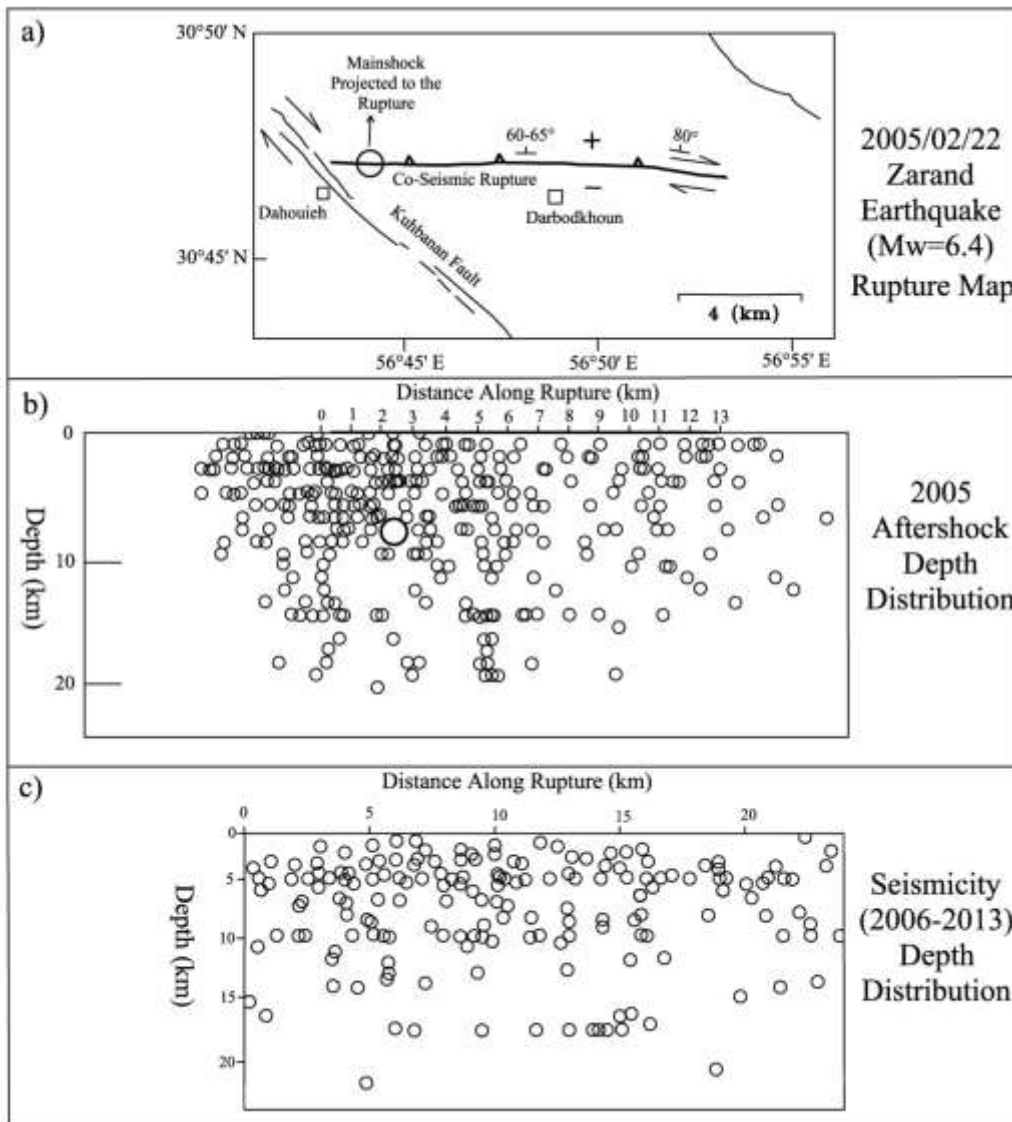


**Figure 10.** a) The 2005 Zarand event co-seismic rupture [37], b) 2005 aftershock sequence [31] and c) microseismicity (IGUT) along 2005 earthquake rupture. The hypocentral area is still empty from microseismicity.

phenomenon in Persia. Fig. 9 shows an area of dense background seismicity (2006-2013 events from the IGUT database) at the southeastern end of the co-seismic fault which is associated with lack of aftershock activity.

Figure 10 shows the 2005 aftershock sequenc and seismicity along the 2005 Zarand earthquake co-seismic rupture. Although, along the Zarand earthquake rupture, an anti-correlation between aftershock activity and subsequent background seismicity is not seen as clearer as the Zirkuh event. About this earthquake we could only say that the hypocentral area is still empty from the

microseismicity.

### Results and Discussion

We examined data of 43 Persian earthquakes which were chosen from 4 different seismotectonic provinces. They have been selected in a relatively wide range of magnitude (5.0-7.7) and also from different mechanisms in order to prevent affection of location and geological parameters on obtained results.

Distance of the largest and furthers aftershocks occurred in a main cluster of aftershocks from a mainshock could be supposed as the rupture length at

depth. Using this method 16.5 km was obtained for the 2005 Zarand earthquake rupture neglecting the scattered and also off-cluster aftershocks. This value is associated with surface rupture length which had been mapped about 13km at the field observations. It confirms that the depth extension of a co-seismic rupture is usually wider than the surface rupture.

In most of the Iranian moderate and large investigated earthquakes, two months aftershock surveying shows an increase of the aftershocks activity with increase in magnitude of the mainshock. Also considering depth of the mainshocks (adapted from body waveform modeling) and the aftershocks surveying with local networks, it reveals that we have a decrease in the aftershock activity with increase in depth of the mainshock.

For most of the Iranian events, the aftershocks affected zone is deeper than depth of the related mainshock (using body waveform modeling for depth determination of the mainshock and also a local network data for depth dispersal of the aftershocks). Hence, we could say that the earthquakes focus are not at the base of seismogenic zone and therefore the events have only broken a part of brittle crust in each area. This is a significant issue in seismic hazard investigations, because, the epicentral area of the earthquakes in Iran are capable of occurring future earthquakes with wider ruptures and therefore an event with greater magnitude could break entire depth of the seismogenic layer.

The earthquakes which occurred on the Caspian fault at north of Iran, have interplate behaviors because they are seen in the lower stress drop area in Kanamori and Anderson, (1975) diagram. Hence it may provide subsidiary confirmation for over thrusting the south Caspian plate.

### Acknowledgement

Thanks to the Institute of Geophysics of the University of Tehran for the seismological data on the website.

### References

- Ashtari M., Hatzfeld D., and Kamalian N. Microseismicity in the region of Tehran. *Tectonophysics*, **395**: 193–208 (2005).
- Atefi S., and Gheitanchi M.R. Investigation of source characteristics of the 1997 Ardabil earthquake. 14<sup>th</sup> Conference of the Geophysics of Iran, *the Institute of Geophysics of the University of Tehran*, 1220-1223 (2000).
- Berberian M. Earthquake faulting and bedding thrust associated with the Tabas-e Golshan Iran earthquake of September 16, 1978. *Bull. Seismol. Soc. Am.*, **69**(6): 1861-1887 (1979a).
- Berberian M. Tabas-e Golshan Iran catastrophic earthquake of September 16, 1978: A preliminary field report. *Disasters*, **2**(4): 207-219 (1979b).
- Berberian M. and Qorashi M. Co-seismic fault-related folding during the south Golbaf earthquake of November 20, 1989, in southeast Iran. *Geology*, **22**: 531–534 (1994).
- Berberian M., Jackson J.A., Qorashi M., Khatib M.M., Priestley K., Talebian M., and Ghafuri-Ashtiani M. The 1997 May 10 Zirkuh (Qa'emat) earthquake (M 7.2): faulting along the Sistan suture zone of eastern Iran. *Geophys. J. Int.*, **136**: 671–694 (1999).
- Berberian M., Qorashi M., Jackson J., Priestley K., and Wallace T. The Roudbar-Tarom earthquake of 20 June 1990 in NW Persia: Preliminary field and seismological observations, and its Tectonic significance. *Bull. Seismol. Soc. Am.*, **82**(4): 1726-1755 (1992).
- Berberian M., Jackson J.A., Qorashi M., Talebian M., Khatib M., and Priestley K. The 1994 Sefidabeh earthquakes in eastern Iran: blind thrusting and bedding-plane slip on a growing anticline, and active tectonics of the Sistan suture zone. *Geophys. J. Int.*, **142**: 283–299 (2000).
- Berberian M., Qorashi M., Jackson J.A., Fielding E., Parsons B.E., Priestley K., Talebian M., Walker R., Wright T.J., and Baker E. The 1998 March 14 Fandoqa earthquake M=6.6 in Kerman, southeast Iran: Re-rupture of the 1981 Sirch earthquake fault, triggering of slip on adjacent thrusts, and the active tectonics of the Gowk fault zone. *Geophys. J. Int.*, **146**(2): 371-398 (2001).
- Berberian M. and Walker R. The Rudbar-Tarom 7.3 earthquake of 1990 June 20; seismotectonics, co-seismic and geomorphic displacements, and historic earthquakes of the western 'High-Alborz', Iran. *Geophys. J. Int.*, doi: 10.1111/j.1365-246X.2010.04705(2010).
- Bhattacharya P., Chakrabarti Kamal, B.K., and Samanta D. Fractal models of earthquake dynamics, Schuster, H.G., (Ed.). *Reviews of Nonlinear Dynamics and Complexity*, Wiley-VCH, Berlin, **2**: 107-158 (2009)
- Byrne D.E., Sykes A.R., and Davis D.M. Great thrust earthquakes and aseismic slip along the plate boundary of the Makran subduction zone. *J. Geophys. Res.*, **97**: 449–478 (1992).
- Donner et al., Segmented seismicity of the Mw 6.2 Baladeh earthquake sequence (Alborz mountains, Iran) revealed from regional moment tensors. *J. Seismol.*, **17**: 925-959 (2013).
- Fatemi J., Akasheh B., and Hamidi G. The 1989/11/20 Golbaf Earthquake and its aftershocks. *Journal of Earth and Space Physics*, University of Tehran, Iran, **24**(1, 2): 11-15 (1998).
- Gao L., Wallace T.C. and Jackson J.A. Aftershocks of the June 1990 Rudbar-Tarom earthquake: Evidence for slip partitioning (Abstract), EOS Trans. Am. Geophys. Un., **72**(44), Fall Meeting suppl. 335 (1991).
- Gheitanchi M.R., and Raeesi M. Analysis of the 1997 Zirkuh (Ghaen-Birjand) aftershock sequence in east-central Iran. *Acta Seismologica Sinica*, **17**(1): 36-48 (2004).
- Gheitanchi M.R., Fatehi A., and Sadikhoy A. Investigations of the February 4<sup>th</sup> 1997 Bojnourd, North-East Iran, earthquake sequence. *J. Earth and Space Physics*, **24**(1, 2): 29-35(1998).

18. Gutenberg B., and Richter C.F. Earthquake magnitude, intensity, energy and acceleration (second paper). *Bull. Seism. Soc. Am.*, **46**: 105-145 (1956).
19. Hosono K., and Yoshida A. On the distribution of epicentral distance between the largest aftershock and the main shock. *Zishin. J. Seismol. Soc. Japan*, **44**: 259–261 (in Japanese) (1991).
20. Hollingsworth J., Jackson J., Alarcon J., Boomer J., and Bolourchi M.J. The 4<sup>th</sup> February 1997 Bojnourd (Garmkhan) earthquake in NE Iran: Teleseismic, and strong-motion evidence for rupture directivity effects on a strike-slip fault. *J. Earthquake Engineering*, **11**: 193-214 (2007).
21. Hessami K., Jamali F., and Tabassi H. Map of Major Active Faults of Iran, Tech. rep. International Institute of Earthquake Engineering and Seismology, Iran, <http://www.iiees.ir> (2003).
22. Jackson J. et al. Seismotectonic, rupture process, and earthquake hazard aspects of the 2003 December 26 Bam, Iran, earthquake. *Geophys. J. Int.*, **166**: 1270-1292 (2006).
23. Kanamori H., and Anderson D.L. Amplitude of the earth's free oscillations and long-period characteristics of the earthquake source. *J. Geophys. Res.*: doi: 10.1029/0JGREA0000800000B8001075000001, (1975).
24. Katsuyuki A., and Kanamori H., Magnitude of great shallow earthquake from 1953 to 1977. *Tectonophysics*, **62**: 191-203 (1980).
25. Lay T., and Wallace T. C. Modern Global Seismology. *Academic Press Institute*, California 92101-4495, ISBN-12-732870-X (1995).
26. Mendoza C., and Hartzell S. Aftershock patterns and main shock faulting. *Bull. Seismol. Soc. Am.*, **78**: 1438 – 1449 (1988).
27. Mogi K. Magnitude-frequency relationship for elastic shocks accompanying fractures of various materials and some related problems in earthquakes. *Bulletin of Earthquake Research Institute*, University of Tokyo, **40**: 831-883 (1962).
28. Moradi-S. A., Hatzfeld D., and Tatar M. Microseismicity and seismotectonics of the North Tabriz fault (Iran). *Tectonophysics*, **506**: 22-30 (2011).
29. Nanjo K., and Nagahama H. Observed correlations between aftershock spatial distribution and earthquake fault lengths. *Terra Nova*, **12(6)**: 312-316 (2000).
30. Nemati M., Hatzfeld D., Gheitanchi M., Sadidkhouy A., and Mirzaei N. Microseismicity and seismotectonics of the Firouzkuh and Astaneh faults (east Alborz, Iran). *Tectonophysics*, **506**: 11-21(2011).
31. Nemati M., and Gheitanchi M. Analysis of 2005 Dahuieh (Zarand) aftershocks sequence in Kerman province. *Journal of Earth and Space Physics*, Geophysics Institute of University of Tehran, Iran, **37(1)**: 1-9 (2011).
32. Nemati M., Hollingsworth J., Zhong W., Bolourchi M. J., and Talebian M. Microseismicity and seismotectonics of the South Caspian Lowlands, northeast of Iran. *Geophys. J. Int.*, doi: 10.1093/gji/ggs114 (2013a).
33. Nemati M., Hollingsworth J., and Ghassemi M.R. Investigation of seismotectonics of eastern south Caspian basin using earthquakes focal mechanism and geomorphological investigations. Geological Survey of Iran, *Earth Science Quarterly Journal*, under press (2013b).
34. Nissen E., Ghorashi M., Jackson J., Parsons P., and Talebian M. The 2005 Qeshm Island earthquake (Iran), a link between buried reverse faulting and surface folding in the Zagros Simply Folded Belt? *Oct. Geophys. J. Int.* **171**: 326-338 (2007).
35. Nissen E., Yamini-Fard F., Tatar M., Gholamzadeh A., Bergman E., Elliott J.R., Jackson J.A., and Parsons B. The vertical separation of mainshock rupture and microseismicity at Qeshm island in the Zagros fold-and-thrust belt, Iran. *Earth and Planetary Science Letters*, **296**: 181-194 (2010).
36. Shahrabi T., and Javan-e Dolouei G. Silakhour Boroujerd plane seismicity characteristics based on local network data. *J. Engineering Geology*, **3(2)**: 697-716 (2009).
37. Talebian M., Biggs J., Bolourchi M., Copley A., Ghassemi A., Ghorashi M., Hollingsworth J., Jackson J., Nissen E., Oveisi B., Parsons B., Priestley K., and Saiidi A. The Dahuieh (Zarand) earthquake of 2005 February, 22 in central Iran. *Geophys. J. Int.*, **164**: 137-148 (2006).
38. Tatar M., Hatzfeld D., and Ghafory-Ashtiany M. Tectonics of the Central Zagros (Iran) deduced from microearthquake seismicity. *Geophys. J. Int.*, **156**: 255-266 (2004).
39. Tatar M., Hatzfeld D., Moradi A.S., and Paul A. The 2003 December 26 Bam earthquake (Iran), M 6.6, aftershock sequence. *Geophys. J. Int.*, **163**: 90-105 (2005).
40. Tatar M., Jackson J., Hatzfeld D., and Bergman E. The 2004 May 28 Baladeh earthquake (Mw 6.2) in the Alborz, Iran: overthrusting the South Caspian Basin margin, partitioning of oblique convergence and the seismic hazard of Tehran. *Geophys. J. Int.*, **170**: 249-261 (2007).
41. Walker R., Jackson J., and Baker C. Surface expression of thrust faulting in eastern Iran: Source parameters and surface deformation of the 1978 Tabas and 1968 Ferdows earthquake sequences. *Geophys. J. Int.*, **152**: 749-765 (2003).
42. Walker R.T., Priestley K., Andalibi M.J., Gheitanchi M.R., Jackson J. A., and Karegar S. Seismological and field observations from the 1990 November 6 Furg (Darab-e Hormozgan) earthquake: a rare case of surface rupture in the Zagros mountains of Iran. *Geophys. J. Int.*, **163**: 567-579 (2005a).
43. Walker R., Bergman E., Jackson J., Ghorashi M., and Talebian M. The 2002 June 22 Changureh (Avaj) earthquake in Qazvin province, northwest Iran: epicentral relocation, source parameters, surface deformation and geomorphology. *Geophys. J. Int.* **160**: 707-720 (2005b).
44. Walker R.T., Bergman E.A., Szeliga, W., and Fielding E.J. Insights into the 1968–1997 Dasht-e-Bayaz and Zirkuh earthquake sequences, eastern Iran, from calibrated relocations, InSAR and high-resolution satellite imagery. *Geophys. J. Int.* doi: 10.1111/j.1365-246X.2011.05213x (2011).
45. Walker R. T., Bergman E. A., Elliott J. R., Fielding E. J., Ghods A.R., Ghorashi M., Jackson J., Nazari H., Nemati M., Oveisi B., Talebian M., and Walters R. J. The 2010-2011 South Rigan (Baluchestan) earthquake sequence and its implications for distributed deformation and earthquake hazard in southeast Iran. *Geophys. J. Int.*, doi: 10.1093/gji/ggs109 (2013).

46. Wessel P. and Smith W.H.F. New improved version of Generic Mapping Tools released, EOS, Trans. *Am. Geophys. Un.* **79(47)**, 579 (1998).
47. Yamini-Fard F., Hatzfeld D., Tatar M., and Mokhtari M. Microearthquake seismicity at the intersection between the Kazerun Fault and the Main Recent Fault (Zagros, Iran). *Geophys. J. Int.*, doi:10.1111/j.1365-246X.2006.02891.x (2006).
48. Yeats R.S. Sieh K.E. and Allen C.R. *The Geology of Earthquakes*. Oxford Press, New York, 568p. (1997).
49. Berberian M. *Contribution to the seismotectonics of Iran, Part II*. Geological Survey of Iran, report No. 39, 516p. (1976).
50. Kosarev A.N. and Kostianiy G. *The Caspian Sea Encyclopaedia*. Springer, 552p. (2010).
51. Scholz C.H. *Mechanics of Earthquakes and Faulting*, Cambridge University Press, Cambridge, 435p. (2002).
52. Rezapour M. Study of mechanism and aftershocks of Roudbar-Manjil earthquake 1991. *Geophysics Institute, University of Tehran, Iran*, M.Sc. thesis (in Persian), 200p. (1991).
53. Harvard University, Department of Geological Sciences, Centroid Moment Tensor catalogue, available online at: <http://www.globalcmt.org/CMTsearch.html>.
54. International Seismological Center, ISC, <http://www.isc.ac.uk>.
55. Institute of Geophysics University of Tehran, IGUT, <http://irsc.ut.ac.ir>.
56. Origin Software, [www.microcal.com](http://www.microcal.com).